

Predicting time-dependent motion in the double-diffusive convection system

H. P. Fang¹ and Z. H. Liu²

¹*China Center of Advanced Science and Technology (World Laboratory), P.O. Box 8730, Beijing 100080, China and Institute of Theoretical Physics, P.O. Box 2735, Beijing, 100080, China**

²*Physics Department, Guangxi University, Guangxi 530004, People's Republic of China*

(Received 7 December 1993; revised manuscript received 6 June 1994)

The relationship between the control parameters for the double-diffusive convection system and those for a one-dimensional map is established with the technique of symbolic dynamics. Then the parameter value for the desired time-dependent motion in the double-diffusive convection system can be predicted.

PACS number(s): 47.27.Te, 47.20.Ky, 47.52.+j, 05.45.+b

I. INTRODUCTION

Convection has matured into a subject with a large variety of applications. Many situations exist in oceanography, astrophysics, and chemical engineering, etc. Consider a fluid layer containing a bottom-heavy distribution of a solute, such as salt as in oceanography, and heated from below. A warmer fluid parcel may raise because of less density, then it comes into a cooler, less salty environment. Because the rate of molecular diffusion of heat is larger than that of salt, the thermal field tends to equilibrate with its surrounding more rapidly than does the salt field. This parcel is then heavier and sinks. A convection may happen. Since there is a phase lag between the thermal diffusion and the solute diffusion, like a spring with a phase difference between the stabilizing force and the destabilizing force, the small amplitude of the convection may grow and becomes more nonlinear. Under some conditions, the convection will exhibit periodic or chaotic motion.

Double-diffusive convection can be realized in the laboratory with cold fresh water lying above hot salty water, or with a dissolved salt-sugar mixture, or with binary fluids (water-ethanol or ²He-³He mixtures) which are even more convenient for experiments [2]. Similar behavior arises in a rotating system or in the presence of a magnetic field.

Idealized double-diffusive convection provides the simplest model problem for these systems naturally or experimentally and has received considerable attention. Most of the theoretical work concentrated on the two-dimensional case. In the Boussinesq approximation with the imposed symmetric lateral boundary conditions, the model possesses discrete spatial symmetry. The solutions of this model may retain or not retain this symmetry, which is called the symmetric solutions and the asymmetric solutions. The asymmetric periodic solutions undergo a cascade of period-doubling bifurcations into chaos. The chaotic region is interspersed with windows containing

more complicated periodic orbits, both symmetric and asymmetric. For the symmetric periodic solutions, the period-doubling bifurcations must be preceded by a bifurcation to asymmetric [3–5]. Their behavior reveals the similarity with that of one-dimensional (1D) mappings [6]. Despite those observations, there has never been a systematic investigation of the bifurcation behavior and the chaotic dynamics on a parameter axis.

So far symbolic dynamics provides the most robust technique to understand systematics of these periodic windows interspersed in chaotic region [7]. In one-dimensional mappings it has been well established that the periodic windows embedded in chaotic region can be ordered and generated in a systematic way according to symbolic dynamics of two or three letters [7]. However, for systems described by differential equations this kind of global property is still less understood. A few years ago, Hao *et al.* had presented approaches towards the understanding of this global property on the Lorenz equations [8] and forced Brusselator [9]. They found many of the periodic windows with short length can fit into the universal form of 1D mappings. The parameters of the systems they discussed, however, are far from the real physical problems. Swinney and co-workers had also applied the symbolic dynamics to the experimental data from the Belousov-Zhabotinskii reaction and found that the periodic orbits interspersed in the chaotic region can be modeled by 1D maps [10]. In this paper, we will apply the symbolic dynamics to the double-diffusive convection system. We first give a quantitative comparison between the systematics of stable periodic windows interspersed in chaotic region of this system with that of 1D mappings with the same antisymmetry. By determining the kneading sequences (which will be defined in Sec. III) of the double-diffusive convection system numerically, the relationship between the control parameters for the double-diffusive convection system and those for a 1D map is then established and the parameter value for the desired time-dependent motion (not restricted to periodic motion) in the double-diffusive convection system can be predicted.

The paper is organized as follows. In Sec. II we review the basic ideas of symbolic dynamics for 1D map-

*Address for correspondence.

pings with antisymmetry. Then in Sec. III we apply the symbolic dynamics to the double-diffusive convection system to predict the parameter value for the desired time-dependent motion. In Sec. IV, we assess the significance and limitations of our study and suggest direction for future research.

II. SYMBOLIC DYNAMICS FOR A 1D ANTISYMMETRIC CUBIC MAP

In this section we will review the basic ideas of the symbolic dynamics for the following 1D antisymmetric cubic map

$$x_{n+1} = F(x_n) = Ax_n^3 + (1 - A)x_n. \quad (1)$$

This map maps the interval $[-1, 1]$ into itself when A varies in $[1, 4]$. The shape is shown in Fig. 1 where \bar{C} and C denote the maximal and minimal points, respectively, which divide the interval $[-1, 1]$ into three monotonic segments marked by L , M , and R . Nearly all trajectories are then unambiguously encoded by infinite strings $S(x) = (s_0 s_1 s_2 \dots)$, s_i may be one of the five letters L, \bar{C}, M, C , and R .

For these symbolic strings, we can define ordering rules referring to the natural order in the 1D interval $[-1, 1]$. It is clear that

$$R > C > M > \bar{C} > L.$$

Let us consider two symbolic strings $S(x_1)$ and $S(x_2)$ from initial points x_1 and x_2 and assume $S(x_1) = P^* \mu_1 \dots$ and $S(x_2) = P^* \mu_2 \dots$, respectively, where P^*

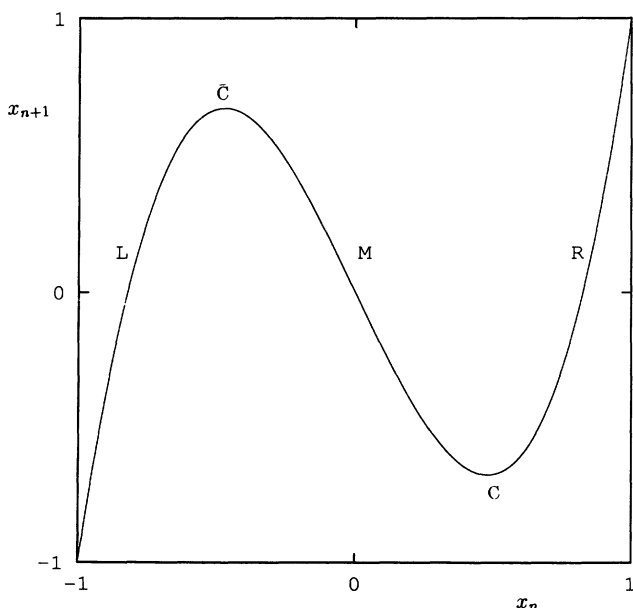


FIG. 1. The shape of the 1D map $x_{n+1} = Ax_n^3 + (1 - A)x_n$. \bar{C} and C denote two critical points which divide the interval $[-1, 1]$ into three monotonic segments marked by L , M , and R .

is the common part and $\mu_1 \neq \mu_2$ are the first different letters which may be L, \bar{C}, M, C , or R . Since only a letter M corresponds to a decreasing monotonic branch (which will reverse the order), we obtain the order for $S(x_1)$ and $S(x_2)$ as follows:

$$\left. \begin{array}{l} S(x_1) > S(x_2) \\ S(x_1) < S(x_2) \end{array} \right\} \text{for } \mu_1 > \mu_2$$

and

$$P^* \text{ contains an } \begin{cases} \text{even} \\ \text{odd} \end{cases} \text{ number of } M\text{'s}.$$

The attractor of the map (1) will always lie in the interval $[F(C), F(\bar{C})]$, e.g., $x \in [F(C), F(\bar{C})]$. Denoted by K_g and K_s the kneading sequences which are the symbolic sequences from \bar{C} and C , we get the admissibility conditions for a word $S(x)$ corresponding to a real orbit of the map (1), which is: $S(x)$ is allowed if and only if it satisfies

$$K_g \geq \sigma^m(S(x)) \geq K_s, \quad m = 0, 1, 2, \dots, \quad (2)$$

where σ is a shift operator. It should be emphasized that the kneading sequences K_g and K_s from the maximal and minimal points play a crucial role in the determination of the topological properties of the 1D map (1) at given parameter A . From the antisymmetric property of the map (1) $K_s = \bar{K}_g$. \bar{K}_g is the conjugate of K_g obtained by interchanging L 's and R 's but leaving M 's unchanged.

It should be mentioned that the symbolic dynamics constructed in this way is independent of a particular mapping. It is universal for all the mappings with two critical points and the antisymmetric property [7,12]. The kneading sequences determine the topology of these systems completely.

Now we consider the property of the 1D map on a parameter axis. Generally, the kneading sequences K_s and K_g will change as A alters. For the map (1), it is found that K_g increases monotonically as A increases. Consequently, from the grammar (2), once an orbit is created, it will always exist as parameter A increases.

When the kneading sequences are periodic strings, the map (1) exhibits stable periodic orbits $[dF(x)/dx = 0 \text{ at } \bar{C}]$, which are called superstable periodic orbits. Consequently, the kneading sequences are called the superstable words. Owing to the antisymmetry, there are two kinds of superstable words. A symmetric superstable periodic word will be of the form

$$\bar{C}(\sigma_1 \sigma_2 \dots \sigma_n C \bar{\sigma}_1 \bar{\sigma}_2 \dots \bar{\sigma}_n \bar{C})^\infty = \bar{C}(PC\bar{P}\bar{C})^\infty,$$

where σ_i is L, M , or R and $\bar{\sigma}_i$ is the conjugate of σ_i . Similarly, an asymmetric superstable word looks like

$$\bar{C}(\sigma_1 \sigma_2 \dots \sigma_n \bar{C})^\infty = \bar{C}(P\bar{C})^\infty.$$

We omit the cycling hereafter as understood and simply call these superstable periodic words $PC\bar{P}\bar{C}$ and $P\bar{C}$.

III. PREDICTING TIME-DEPENDENT CONVECTION IN THE DOUBLE-DIFFUSIVE CONVECTION SYSTEM

The model of Veronis [11] for the double-diffusive convection is based on permeable, free-slip horizontal boundary conditions. Assuming that the standing waves were the only relevant oscillating structure, he introduced the minimal truncated five-mode model as follows [11]

$$\begin{aligned} \dot{a} &= \sigma(-a + r_T b - r_S d), \\ \dot{b} &= -b + a(1 - c), \\ \dot{c} &= \bar{w}(-c + ab), \\ \dot{d} &= -\tau d + a(1 - e), \\ \dot{e} &= \bar{w}(-\tau e + ad), \end{aligned} \tag{3}$$

where dots indicate differentiation with respect t . a, b, d measure the amplitude of first-order perturbations to the stream function, temperature, and solute concentration, respectively, while c and e are measures of the second-order thermal and solutal perturbations. The parameters r_T and r_S are normalized thermal and solutal Rayleigh numbers, σ is the Prandtl number, τ ($0 < \tau < 1$) is the ratio of the solutal to the thermal diffusivity, and \bar{w} ($0 < \bar{w} < 4$) is a geometrical factor, related to the width of a convection cell.

This five-mode system reproduces the features of the full double-diffusive convection system qualitatively and even quantitatively when the convection (or a, b, c, d, e) is sufficiently small [11].

The system (3) is invariant under the transformation

$$a \rightarrow -a, b \rightarrow -b, c \rightarrow c, d \rightarrow -d, e \rightarrow e,$$

in which the variable a shares the same discrete symmetry as x in the map (1). In this section we will study the universal behavior of this five-mode equations with the symbolic dynamics for the antisymmetric map (1). We use a fourth-order Runge-Kutta scheme with appropriately chosen time steps. The parameter values are set at $\sigma = 10, \tau = 0.4, \bar{w} = 8/3, r_S = 6$.

Equations (3) may have five fixed points. When the trivial solution with $a = b = c = d = e = 0$ becomes unstable at $r_T^H = 1 + (1 + \sigma + \tau)\frac{\tau}{\sigma} + \frac{(\sigma + \tau)}{(\sigma + 1)} \approx 7.1255$, a stable symmetric periodic orbit arises. After a symmetry-breaking bifurcation at $r_T = 7.782$, and a series of period-doubling bifurcations, the system becomes chaotic. It is found that all the interesting trajectories intersect the plane $c = 0.17$ from $r_T = 7.4$ upwards. We call this plane Σ and reduce Eqs. (3) to the map (called F) in this Poincaré section Σ .

The symbolic system we use is based on the first return map in Figs. 2(a), 2(b) for $r_T = 7.797$ and $r_T = 7.796247$. Figures 2(a), 2(b) are obtained by plotting the successive a_{n+1} versus a_n of the map F . These return maps both reveal an outline of the underlying 1D mapping, see, e.g., Fig. 1 [the deviations from a 1D map in Fig. 2(a) will be discussed later]. It is remarkable that Fig. 2(b) looks very similar to what one would get for an asymmetric period 10 orbit from Fig. 1. We obtained similar plottings for other periodic windows. This obser-

vation is crucial for all the subsequent discussions and suggests a reasonable way to name the periodic windows in the double-diffusive convection model by words following the same rules of that for map (1). This fact implies that the dynamics underlying the overall periodic structure may be understood in the light of 1D mappings. As that of the 1D mapping (1), we identify [7] the largest numerical output x_i as the left critical point \bar{C} , then all other x_i 's acquire a unique assignment of letters L, M, R , or C . We show this process in Table I for the period 10 orbits at $r_T = 7.796247$.

We present our results in Table II in which all the periodic windows discovered are listed in increasing r_T

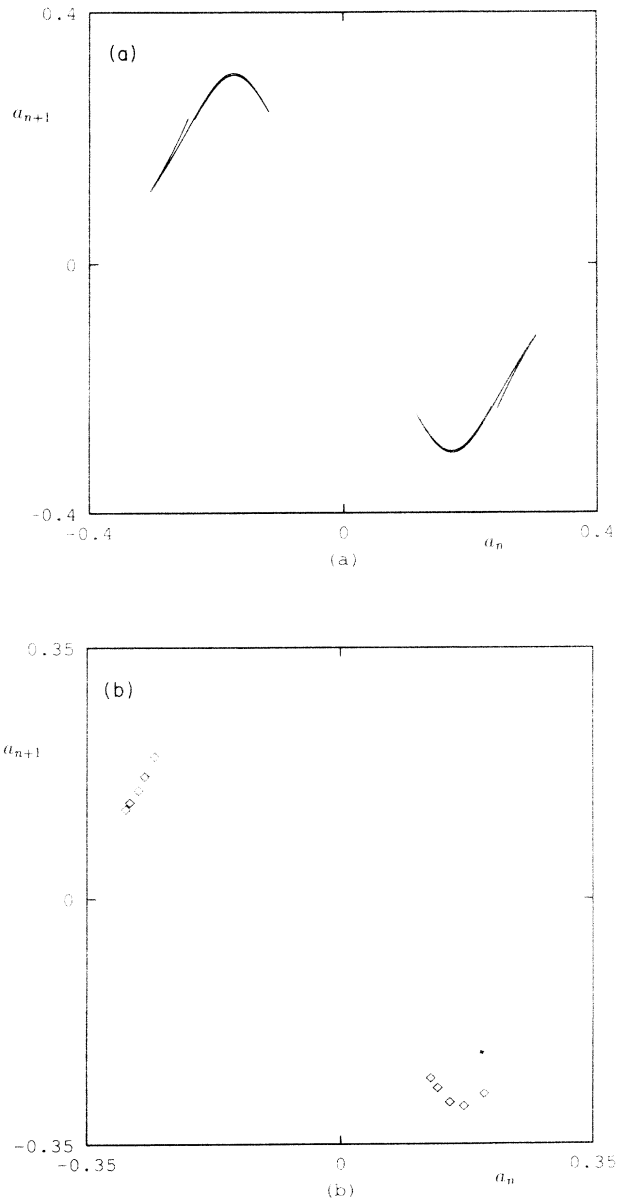


FIG. 2. The first return map of the double-diffusive convection system (1) in Σ . (a) $r_T = 7.797$ (chaotic orbit); (b) $r_T = 7.796247$ (asymmetric period 10 orbit).

TABLE I. Assignment of letters to a period 10 orbit at $r_T = 7.796\ 247$.

-0.1710	0.2963	-0.1252	0.2564	-0.1985	0.2788	-0.1516	0.2908	-0.1349	0.2703
\bar{C}	R	M	R	L	R	M	R	M	R

order along with their periods, words, and locations on the parameter axis. Here the period is defined as the period of the map F which equals the number of points in Σ . We also list the value of A for each word in the 1D mapping (1). These results clearly show that all of the 10 periodic windows can fit into the 1D cubic scheme. The most remarkable observation from Table II is the order of all the words being exactly the same as that of their 1D counterpart along the increasing A direction. Let us take $P_1 = RMRLRMRRMRMR\bar{C}$ at $r_{T_1} = 7.796\ 078$ and $P_2 = RMRLRMRRMR\bar{C}$ at $r_{T_2} = 7.796\ 247$ as examples. According to the 1D map (1), $A_{P_1} = 3.317\ 412$ and $A_{P_2} = 3.321\ 906$. $A_{P_1} < A_{P_2}$ corresponds to $P_1 < P_2$ and $r_{T_1} < r_{T_2}$. We emphasize that the parameter r_T in the double-diffusive convection model is in a sense the same as the parameter A in the cubic map (1). Therefore, increasing r_T is the same as increasing A . The perfect ordering reflects the fact that double-diffusive convection system shares the same topological universal properties with the 1D cubic map (1).

The similarity between the topology of the double-diffusive convection and the 1D antisymmetric cubic map (1) is not restricted to the periodic oscillations. For the chaotic convection we get the same observations. For the first return map of the Eqs. (3), as that in the 1D map (1), the kneading sequences K_g can be calculated numerically from the maximal a value for a given r_T . The calculated K_g corresponds to an A value in the 1D map (1). Then the relationship between the parameter r_T in the double-diffusive convection system and the parameter A in the 1D map (1) is established, which is shown in Fig. 3. The platforms interspersed in this r_T - A relationship represent the periodic windows. From this relationship, the parameter r_T for desired time-dependent convection can be predicted. For example, if one wants

the double-diffusive convection system to exhibit period-10 oscillations with a word $RMRLRMRRMR\bar{C}$, which corresponds to $A = 3.321\ 906$ in the 1D map (1), we get $r_T \approx 7.796\ 24$ from Fig. 3. After a more careful searching we find the period-10 oscillations with a word $RMRLRMRRMR\bar{C}$ at $r_T = 7.796\ 247-7.796\ 250$. With a more powerful computer, we can compute the r_T - A relation to very high accuracy. Then the r_T value for the period-10 oscillations with a word $RMRLRMRRMR\bar{C}$ in the double-diffusive convection system can be “read” directly from Fig. 3, and so this also applies for other desired periodic convection whenever it exists.

Now we consider the deviations from a 1D map in the first return map shown in Fig. 2(a) (in some part the map becomes double valued). Due to the complexity of the five-mode Eqs. (3), we cannot expect the first return map in Fig. 2(a) to be completely one dimensional. In order to reveal the complex topological property of the first return map in Fig. 2(a), we have to study it with symbolic dynamics for 2D mappings with antisymmetry [14]. In the present paper, we will not detail them anymore and only present the results. It is remarkable to find that the results are just those obtained above with the symbolic dynamics for 1D mappings when we only consider the periodic orbits with period < 20 . Thus the technique used above is a robust and practical one and we do not need to bother about the double valuedness in the first return maps.

IV. CONCLUSION AND DISCUSSIONS

We have applied symbolic dynamics to the real physical model on a parameter axis. This allows us to establish the relationship between the control parameters for the

TABLE II. Periodic windows for the model (3) with $\sigma = 10$, $\tau = 0.4$, $\bar{\omega} = 8/3$, and $r_S = 6$. “*” denotes the orbit after the symmetry-breaking bifurcation. The symmetric words are included in the parentheses.

No.	Period	Word	A	r_T range
1	2*	$R\bar{C}$ ($C\bar{C}$)	3.121320	7.1255–7.7921
	4	$RM\bar{R}\bar{C}$	3.262879	7.7922–7.7948
	8	$RMRLRM\bar{R}\bar{C}$	3.293843	7.7949–7.79545
	16	$RMRLRMRRMRRLRM\bar{R}\bar{C}$	3.300475	7.79546–7.79548
2	24	$RMRLRMRRMRRLRMRLRMRLRM\bar{R}\bar{C}$	3.303736	7.795544–7.795545
3	20	$RMRLRMRRMRRLRMRLRM\bar{R}\bar{C}$	3.306480	7.795650–7.795659
4	12	$RMRLRMRRMR\bar{R}\bar{C}$	3.309068	7.795740–7.795759
5	20	$RMRLRMRRMRMRMRRLRM\bar{R}\bar{C}$	3.311313	7.795840–7.795849
6	16	$RMRLRMRRMRMRMR\bar{R}\bar{C}$	3.313043	7.795901
7	14	$RMRLRMRRMRMR\bar{R}\bar{C}$	3.317412	7.796078–7.796081
8	10	$RMRLRMRRMR\bar{R}\bar{C}$	3.321906	7.796247–7.796250
9	14*	$RMRLRLMLRLRL\bar{R}\bar{C}$ ($RMRLRLCLMLRL\bar{R}\bar{C}$)	3.373058	7.797381
10	10*	$RMRLMLLR\bar{R}\bar{C}$ ($RMRLCLMLLR\bar{R}\bar{C}$)	3.394393	7.797924–7.797994

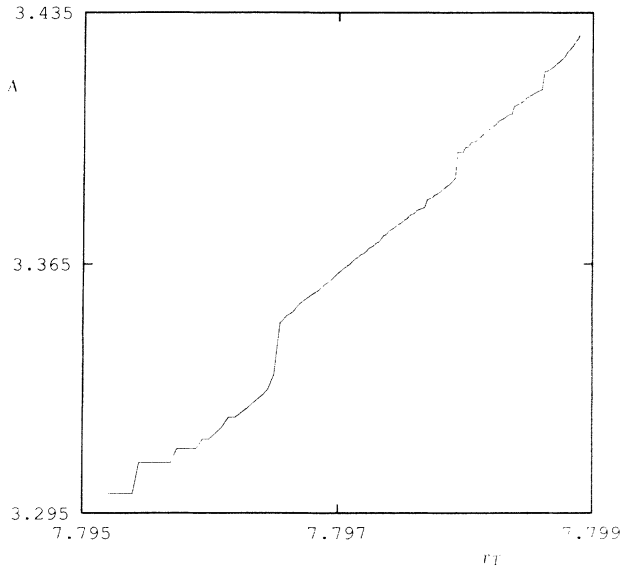


FIG. 3. The relationship between r_T for the double-diffusive convection system and A for the 1D map (1).

physical model with those in the underlying 1D mapping. Since the behavior for 1D maps has been well understood, the control parameter for the desired convection can be well predicted. These results are helpful to control the motion of the double-diffusive convection fluid systems (by changing the relevant conditions) both naturally or experimentally. To our knowledge, this is the first example to establish the one-to-one relationship between the control parameters for the physical model with those in a well-known 1D mapping in a wide range of parameters by calculating the kneading sequences of the first return maps of the physical system numerically and then the parameter for the desired convection (not only restricted to the periodic motion) can be well predicted.

The technique and results in the present paper also help to make the technique of “controlling chaotic dy-

namical system” [13] be more available. Recently, much attention has been paid on stabilizing a desired unstable orbit. However, the desired unstable orbit may not exist in some parameters. For example, $K_g < RMRLRMRC$ for $R_T < 3.321906$. The periodic motion denoted by $RMRLRMRLC$ is not allowed from the grammar (2) for $R_T < 3.321906$ in the double-diffusive convection system. With our method we can predict the parameter range for the desired time-periodic motion embedded in the chaotic orbit and then it can be stabilized. For the periodic motion denoted by $RMRLRMRLC$, it can only be found and stabilized for $R_T > 3.321906$.

It should be noted that the model considered in the present work is an idealized one with free-slip-permeable boundary conditions which are not the physically relevant ones. However, this model does provide the simplest model problem for these systems naturally or experimentally which is easy to discuss in detail. We are encouraged that the technique presented in this paper can also apply to predicting the time-dependence motion of real physical fluid systems with experimental boundary conditions. It also should be noted that the traveling waves [15] usually coexist with the standing waves in fluid systems and we only discuss the standing waves in the present paper. The work on the application of the symbolic dynamics to predicting time-dependence motion of real physical fluid systems both for standing waves and traveling waves is still to be undertaken.

ACKNOWLEDGMENTS

The authors sincerely thank Professor Hao Bai-lin for his encouragement. They also thank Professor E. Knobloch, and Dr. D. R. Moore for providing recent publications and manuscripts of unpublished work. This work was partially supported by a grant from CNSF, and by the Computer Center of the ITP which provides us with SUN workstation time.

- [1] H. Stommel, A. B. Arons, and D. Blanchard, *Deep Sea Res.* **3**, 152 (1956).
- [2] E. Kaplan and V. Steinberg, *Phys. Rev. E* **48**, R661 (1993).
- [3] L. N. Da Costa, E. Knobloch, and N. O. Weiss, *J. Fluid Mech.* **109**, 25 (1981); W. Schöpt and W. Zimmermann, *Phys. Rev. E* **47**, 1739 (1993).
- [4] E. Knobloch, M. R. E. Proctor, and N. O. Weiss, *J. Fluid Mech.* **239**, 273 (1992).
- [5] James W. Swift and Kurt Wiesenfeld, *Phys. Rev. Lett.* **52**, 705 (1984).
- [6] D. R. Moore and N. O. Weiss, *Philos. Trans. R. Soc. London Ser. A* **332**, 121 (1990); M. R. E. Proctor and N. O. Weiss, *Nonlinearity* **3**, 619 (1990).
- [7] Hao Bai-lin, *Elementary Symbolic Dynamics and Chaos in Dissipative Systems* (World Scientific, Singapore, 1989).
- [8] M. Z. Ding and B. L. Hao, *Commun. Theor. Phys.* **9**, 375 (1988).
- [9] B. L. Hao, *Physica A* **104**, 85 (1986).
- [10] R. H. Simoyi, A. Wolf, and H. L. Swinney, *Phys. Rev. Lett.* **49**, 245 (1982); K. Coffman, W. D. McCormick, and H. L. Swinney, *ibid.* **56**, 999 (1986).
- [11] G. Veronis, *J. Mar. Res.* **23**, 1 (1965).
- [12] N. Metropolis, M. Stein, and P. Stein, *J. Combinat. Theor. A* **15**, 25 (1973).
- [13] E. Ott, C. Grebogi, and J. A. Yorke, *Phys. Rev. Lett.* **64**, 1196 (1990).
- [14] H. P. Fang, *J. Phys. A* (to be published).
- [15] S. J. Linz and M. Lücke, *Phys. Rev. A* **35**, R399 (1987); G. Ahlers and M. Lücke, *ibid.* **35**, R470 (1987); M. C. Cross, *Phys. Lett. A* **119**, 21 (1986).